

---

# LLaVA-CMoE: Towards Continual Mixture of Experts for Large Vision-Language Models

---

Hengyuan Zhao<sup>1\*</sup>, Ziqin Wang<sup>1\*</sup>, Qixin Sun<sup>1\*</sup>, Kaiyou Song, Yilin Li,  
Xiaolin Hu<sup>2†</sup>, Qingpei Guo<sup>†</sup>, Si Liu<sup>1†</sup>

<sup>1</sup>School of Artificial Intelligence, Beihang University

<sup>2</sup>Tsinghua University

## Abstract

Mixture of Experts (MoE) architectures have recently advanced the scalability and adaptability of large language models (LLMs) for continual multimodal learning. However, efficiently extending these models to accommodate sequential tasks remains challenging. As new tasks arrive, naive model expansion leads to rapid parameter growth, while modifying shared routing components often causes catastrophic forgetting, undermining previously learned knowledge. To address these issues, we propose **LLaVA-CMoE**, a continual learning framework for LLMs that requires no replay data of previous tasks and ensures both parameter efficiency and robust knowledge retention. Our approach introduces a Probe-Guided Knowledge Extension mechanism, which uses probe experts to dynamically determine when and where new experts should be added, enabling adaptive and minimal parameter expansion tailored to task complexity. Furthermore, we present a Probabilistic Task Locator that assigns each task a dedicated, lightweight router. To handle the practical issue that task labels are unknown during inference, we leverage a VAE-based reconstruction strategy to identify the most suitable router by matching input distributions, allowing automatic and accurate expert allocation. This design mitigates routing conflicts and catastrophic forgetting, enabling robust continual learning without explicit task labels. Extensive experiments on the CoIN benchmark, covering eight diverse VQA tasks, demonstrate that LLaVA-CMoE delivers strong continual learning performance with a compact model size, significantly reducing forgetting and parameter overhead compared to prior methods. These results showcase the effectiveness and scalability of our approach for parameter-efficient continual learning in large language models. Our code will be open-sourced soon.

## 1 Introduction

Multimodal large language models (MLLMs) [4, 61, 34, 48, 37] have demonstrated remarkable capabilities in understanding and generation across multiple modalities. Following large-scale pre-training, these models typically require further adaptation to perform effectively on specific downstream tasks. To enable efficient adaptation without necessitating full model retraining, Parameter-Efficient Fine-Tuning (PEFT) methods [1, 20, 24, 23, 39, 40, 16, 66, 9] are widely adopted. These methods ensure computational efficiency and scalability while achieving competitive task-specific performance.

Currently, MLLM training is commonly conceptualized as a multi-task learning (MTL) paradigm where all tasks' data are simultaneously accessible. However, in real-world scenarios, knowledge and tasks are continuously updated in a streaming manner, posing new challenges for the efficient

---

\*Equal Contribution

†Corresponding author

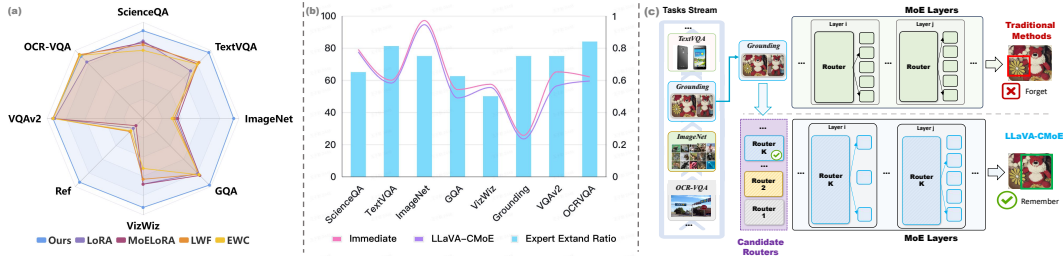


Figure 1: **a) Visualization of the Model’s Anti-Forgetting Capability.** Our method significantly improves anti-forgetting capability, achieving a performance boost of approximately X% compared to baselines. **b) Model Forgetting Ratio vs. Parameter Expansion Rate.** *Immediate* means the performance just after training. When training on task streams, our methods nearly match the performance of *Immediate* while saving nearly 30% parameters, enhancing efficiency. **c) Conceptual comparison between the previous method and our LLaVA-CMoE.** Unlike traditional methods that use a fixed number of experts, our model dynamically adjusts experts per layer based on task needs. Besides, we also build a router bank to reduce forgetting and improve knowledge retention. For clarity, we illustrate only the routing and experts within the block.

adaptation of MLLMs. This dynamic environment necessitates that fine-tuning methods not only remain parameter-efficient, but also support robust continual learning (CL) to enable models to incrementally acquire new knowledge from new tasks, without access to data from previous tasks.

Catastrophic forgetting [30, 11], a fundamental issue in CL, also poses a significant challenge for achieving efficient continual learning in MLLMs. To address this issue, some approaches [6, 32, 63] involve storing data from previous tasks as subsets or distributions, and utilize a data replay scheme during new tasks training to prevent knowledge forgetting. However, as tasks multiply, the storage and computational overhead associated with replay-based methods can become prohibitive. Another line of works [31, 68, 17, 70, 12, 52, 25, 5, 57, 22, 44, 63] focuses on designing novel loss functions or model architectures to alleviate forgetting. Nonetheless, these approaches typically involve updating parameters shared across tasks, which may still lead to performance degradation on previously learned tasks due to interference.

Recently, Wang et al. [59] proposed leveraging a Mixture of Experts (MoE) architecture by introducing new experts at all layers to acquire task-specific knowledge during continual learning. While the scalability of MoE architectures makes them a promising framework for continual learning, two major challenges remain: 1) *When and where should experts be inserted?* Existing study [64] shows that the number of additional parameters required varies significantly across tasks, suggesting that expert allocation should be adaptively determined by task similarity rather than statically predefined. To address this, [69] investigates dynamic expert allocation by analyzing changes in expert selection distributions before and after task training. However, such distributional shifts mainly reflect changes in task preference, rather than a genuine need for new experts. As a result, current approaches may struggle to accurately determine when and where new experts are truly needed for effective continual learning. 2) *How to mitigate catastrophic forgetting in the Router?* In MoE architectures, the Router is a crucial component responsible for dynamic expert allocation. While optimizing experts for new tasks may lead to forgetting previously acquired knowledge, fine-tuning the Router can also alter the routing strategies for earlier tasks, similarly resulting in catastrophic forgetting. [65] addresses this by fixing the number of experts and continuously adding routers to ensure the integrity of the knowledge in previous routers. However, as the number of tasks increases, maintaining a fixed set of experts may limit the model’s capacity to accommodate tasks with substantial differences.

Building on the aforementioned challenges in expert allocation and the mitigation of catastrophic forgetting, we propose an effective framework, **LLaVA-CMoE**, which requires no replay data while enabling truly continual learning. Our method facilitates adaptive parameter updates, enabling the network to autonomously determine when and where updates are necessary. These updates ensure that all previously acquired knowledge remains intact during the learning of new tasks. To tackle the challenge in expert allocation, we propose the **Probe-Guided Knowledge Extension (PGKE)** algorithm, which leverages a small amount of probe data from new tasks to monitor the behavior of experts newly added at each layer. Each expert functions as a probe; by observing the activation frequency of each expert probe, the network is able to independently determine whether additional parameters are required at each layer, avoiding unnecessary parameter growth in [69]. To address the

challenge of catastrophic forgetting, we introduce the **Probabilistic Task Locator (PTL)** strategy. Rather than relying on a single shared router, which is susceptible to routing conflicts across tasks, we assign each task its own dedicated router. This design ensures that the knowledge and routing preferences for previous tasks can be preserved, as activating the corresponding router enables full recovery of prior performance. Since routers are lightweight compared to experts, this approach adds minimal computational overhead. However, during inference, the task identity is typically unknown and inputs are presented in a task-agnostic manner. To effectively identify the appropriate router for each input, we draw inspiration from [46, 45, 2] and employ a reconstruction-based strategy. Specifically, we learn task-specific distributional representations under a VAE-based framework. During inference, the model evaluates the reconstruction error across all tasks and selects the one that best matches the input distribution. This enables PTL to autonomously infer the task category and dynamically route inputs to the most suitable experts, ensuring robust performance across diverse and unknown tasks.

We evaluate LLaVA-CMoE on the CoIN dataset [7], a benchmark tailored to assess continual learning performance across eight distinct VQA-based tasks. Through extensive quantitative and qualitative evaluations, along with comprehensive ablation studies, we demonstrate that our approach not only significantly mitigates catastrophic forgetting, but also promotes effective knowledge transfer and adaptation as new tasks are learned sequentially.

## 2 Related Work

**Continual Learning.** Continual learning aims to mitigate catastrophic forgetting [21, 62] and enable incremental knowledge acquisition. Existing methods fall into four main categories: 1) *Regularization-based* approaches [31, 68, 17, 70], which constrain updates to important parameters; 2) *Architecture-based* approaches [12, 52, 25, 5, 57, 22, 44, 63, 65, 8], which add task-specific components to reduce interference; 3) *Replay-based* approaches [6, 32, 63, 41], which store or generate samples for rehearsal; and 4) *Prompt-based* methods [60, 47, 15, 67], which use learnable prompts to maintain performance. However, computational and storage burdens, as well as forgetting due to parameter updates, remain open challenges [7].

**Mixture of Experts.** The Mixture of Experts (MoE) architecture [49, 54, 43] employs specialized expert networks and a gating mechanism for efficient computation. Sparsely-gated MoE [53, 33] has shown strong performance in LLMs, such as Mixtral 8x7B [26], across diverse NLP tasks. Recent work [38, 64, 10, 42] combines MoE with LoRA [24] for more efficient training. MoE’s scalability has led to its adoption in continual learning, e.g., LEMoE [59] adds experts at all layers for new tasks, and Lifelong-MoE [8] trains new experts while freezing old ones. CoIN [7] further explores MoELoRA, but existing methods still face parameter overhead and suboptimal robustness.

**Large Language Models & PEFT.** Recently, Large Language Models [37, 58, 13, 3] have garnered widespread attention for their remarkable abilities in areas such as language generation, in-context learning, and reasoning. To enable data- and compute-efficient adaptation for specific downstream tasks, various Parameter-Efficient Fine-Tuning (PEFT) methods [27, 23, 35] have been introduced. Among these, LoRA [24] stands out by representing weight updates through low-rank decomposition with two matrices, keeping the original weights frozen while training only the new update matrices. In this study, we combined LoRA with MoE for efficient continual MLLM fine-tuning.

## 3 Methodology

In this section, we first clarify the problem formulation of multimodal continual learning in Section 3.1. We then elaborate on the proposed **LLaVA-CMoE** and its core components: Probe-Guided Knowledge Expansion (PGKE) and Probabilistic Task Locator (PTL) in Section 3.2. Finally, we detail the training objectives in Section 3.3.

### 3.1 Problem Formulation

Let  $\{\mathcal{T}_1, \dots, \mathcal{T}_N\}$  be a set of  $N$  tasks, where each task  $\mathcal{T}_i$  has its training set  $\mathbf{D}^i$  consisting of  $n_i$  multimodal inputs  $\mathbf{X} \in \{\mathbf{X}_t^i, \mathbf{X}_{img}^i, \mathbf{X}_l^i\}_{i=1}^{n_i}$ . Here,  $\mathbf{X}_t^i$ ,  $\mathbf{X}_{img}^i$ , and  $\mathbf{X}_l^i$  represent the textual input (instruction), image, and the corresponding answer, respectively. In Continual Learning (CL), the

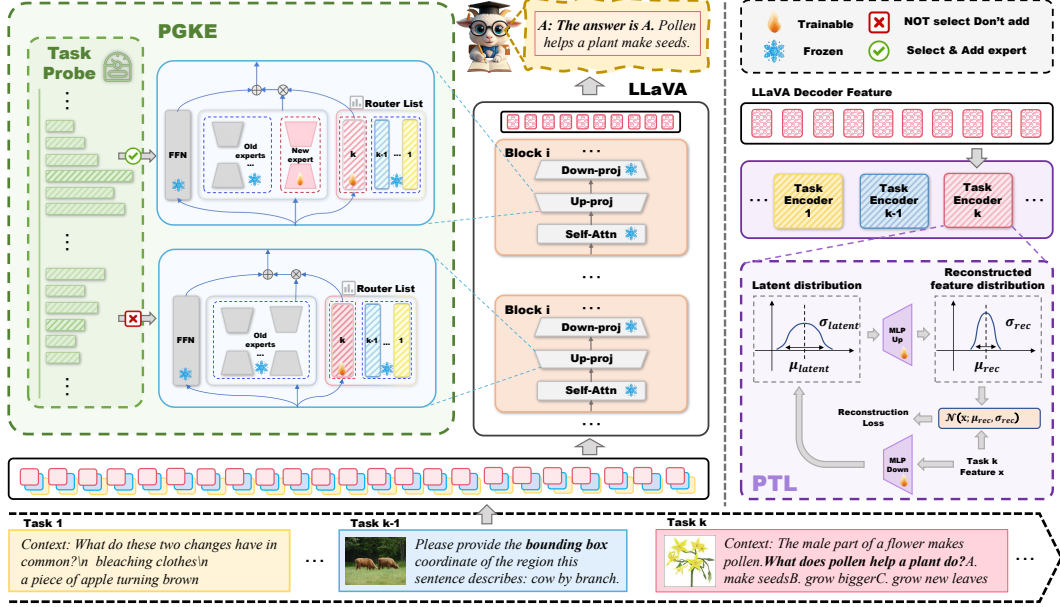


Figure 2: **Overview of our LLaVA-CMoE.** Our model consists of two main components: 1) **Probe-Guided Knowledge Expansion (PGKE)** adaptively allocates the number of experts for different tasks based on task probe guidance, enabling efficient task learning. 2) **Probabilistic Task Locator (PTL)** establishes the connection between task distributions and task routing. During inference, it identifies the corresponding router based on the input, ensuring accurate task-specific processing.

model is trained sequentially on the  $N$  tasks, and while training the  $i$ -th task  $\mathcal{T}_i$ , the model needs to maximize the probability  $P_i$  through Next Token Prediction. Notably, while training the  $i$ -th task, it cannot access to the data of previous tasks  $\{\mathcal{T}_1, \dots, \mathcal{T}_{i-1}\}$ . During the inference phase, we receive only task-agnostic data from either seen or unseen tasks. This practical constraint differentiates our approach from traditional task-incremental learning (Task-IL) paradigms, where explicit task identifiers are typically accessible during inference [55], thus significantly enhancing practical applicability in real-world scenarios where task boundaries may be ambiguous.

### 3.2 LLaVA-CMoE

In this paper, we propose **LLaVA-CMoE**, a framework that enables efficient expert expansion while maintaining strong anti-forgetting capabilities, as illustrated in Figure 2. First, in Section 3.2.1, we introduce the core architecture of the Mixture of Experts framework. Next, in Section 3.2.2, we detail our PGKE mechanism, which dynamically identifies optimal locations for expert expansion. Finally, Section 3.2.3 describes the PTL mechanism, which allows the model to effectively route inputs to task-relevant experts during inference, ensuring comprehensive knowledge utilization.

#### 3.2.1 Mixture of Expert Layer

Our model is built upon a multimodal large language model (MLLM), such as LLaVA [37], in which the Mixture of Experts (MoE) is implemented by augmenting the Feed-Forward Network (FFN) modules within each Transformer block. Furthermore, each expert is constructed using a LoRA-style module, parameterized by  $\{\mathbf{A}_i, \mathbf{B}_i\}_{i=1}^{N_e}$ , where  $N_e$  denotes the number of experts. In the  $h$ -th block, given the multimodal token  $\mathbf{X}_h$ , the output token  $\mathbf{X}_h^{out}$  is computed as follows:

$$\mathbf{X}_h^{out} = \mathbf{W}_0 \mathbf{X}_h + \sum_{i=1}^{N_e} \omega'_i \mathbf{B}_i \mathbf{A}_i \mathbf{X}_h, \quad \omega'_i = \frac{\omega_i}{\sum_{j=1}^{N_e} \omega_j}, \quad \omega_i = \exp(\mathbf{G} \mathbf{X}_h) \cdot \mathbb{I}[i \in \text{topk}(\mathbf{G} \mathbf{X}_h)], \quad (1)$$

where  $\mathbf{W}_0$ ,  $\mathbf{G}$  represent the linear layers' weights of the Feed-Forward Network and the router network, respectively.  $\mathbb{I}$  denotes the indicator function.

### 3.2.2 Probe-Guided Knowledge Extension (PGKE)

Current MoE continual learning methods usually append a *fixed* number of experts to every layer [59, 64] when training a new task. However, simply appending a fixed number of experts to *every* MoE layer after each task (i) wastes parameters when the new task is similar to previous ones, (ii) scales quadratically with the number of tasks, and (iii) still alters the shared router, inducing forgetting. To address these issues, we propose Probe-Guided Knowledge Extension (PGKE), **measuring where the current model lacks capacity before it allocates new experts**. The key intuition is that, if the features required by the incoming task already lie in the span of existing experts, then a freshly initialized “probe” expert will rarely be selected. Conversely, persistent high probe activations indicate that *no existing expert can explain the new examples*, indicating that extra capacity is truly needed. This “try-before-you-buy” principle keeps the parameter budget tight and aligns expansion with genuine knowledge gaps.

Following this principle, we design a two-stage training framework, consisting of *probe locating* and *expert expansion*. Given the training set  $\mathbf{X}^i$  for the  $i$ -th task, we begin by sampling two non-overlapped subsets:  $\mathbf{X}_{\text{train}}^i$  for training and  $\mathbf{X}_{\text{eval}}^i$  for evaluation of the probe experts.

**Probe locating.** In this phase, each MoE layer is augmented by introducing new probe experts along with a corresponding probe router, denoted as  $\mathbf{R}_i$ . To ensure accurate probing,  $\mathbf{R}_i$  is initialized with the parameters of the router from the  $(i - 1)$ -th task, new probe experts are initialized with average weight of old expert group. An additional dedicated sub-router is appended to accommodate the probe experts. During this phase, the parameters of all existing experts are frozen; only the parameters of the probe experts and  $\mathbf{R}_i$  are updated using  $\mathbf{X}_{\text{train}}^i$ .

Upon completion of probe training, we evaluate the activation statistics of all experts in each layer over the validation set  $\mathbf{X}_{\text{eval}}^i$  by computing both the mean and variance of their activation frequencies (logit values). Based on these statistics, we define a threshold for expert expansion as follows (with the layer index omitted for clarity):

$$\text{Threshold} = \text{mean}(\mathbf{Act}) - \alpha \cdot \text{std}(\mathbf{Act}), \tag{2}$$

where  $\alpha$  is a hyperparameter that modulates the sensitivity of expert growth (set to 0.8). If the activation frequencies of  $N_s$  probe experts exceed this threshold, we interpret this as evidence that the current layer requires additional capacity, and therefore augment the layer by introducing  $N_s$  new experts accordingly. The selection process is illustrated in Figure 3.

**Expert expansion.** After determining the optimal number of experts to be integrated into each layer, we perform expert expansion by augmenting the selected layers with the corresponding number of newly initialized experts and routers, following the same initialization strategy as for  $\mathbf{R}_i$ . Additionally, the weights of the new expert are derived from the weights of the expert that is most frequently activated during the probe locating process. Subsequently, the model is fine-tuned on the entire training dataset  $\mathbf{X}^i$ , freezing old experts to mitigate forgetting. To accommodate the varying complexities of different tasks, the parameter  $N_s$ , representing the number of newly added experts, is treated as a dynamically adjustable quantity. This approach not only enhances the efficiency of parameter expansion, but also ensures that the model can effectively adapt to and learn from tasks with greater complexity. A comprehensive analysis of its impact is also presented in Section 4.3.

### 3.2.3 Probabilistic Task Locator (PTL)

After continual learning, most MoE methods fall back to one shared router that tries to satisfy all tasks. Because the router is fine-tuned on the last task, its decision boundary therefore drifts towards the most recent data, so earlier tasks are progressively mis-routed and forgotten. Keeping one dedicated

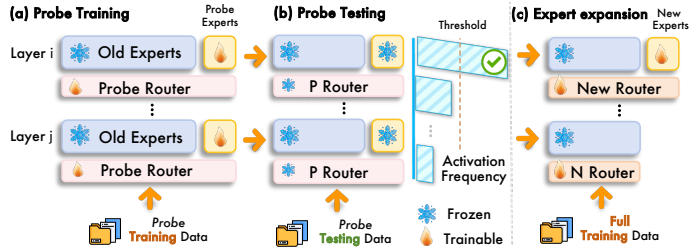


Figure 3: Illustration of Probe-Guided Knowledge Extension (PGKE) process. a) Probe experts are added to all layers. We use probe training data to train probe experts and probe routers. b) Calculating activation frequencies to select layers to expand. c) Expanding selected layers’ experts and doing full training.

router per task (enabled by PGKE) would solve this, but we must know *which* router to activate at test time when task labels are absent. Training an additional classifier to predict task IDs either (i) requires storing replay data or (ii) depends on fragile hand-crafted rules.

Drawn inspiration from [46, 45, 2], we propose the **Probabilistic Task Locator (PTL)**, a *replay-free* mechanism that automatically selects the correct router at inference. The hidden representation of each multimodal input is regarded as a sample from a task-specific distribution; PTL fits this distribution with a light VAE and later measures how well a test sample conforms to each task.

**Task-wise VAE fitting.** For the  $i$ -th task, we pass the input through the frozen LLaVA and fetch the last-token feature  $\mathbf{F}_{\text{end}}$ . The VAE encoder projects  $\mathbf{F}_{\text{end}}$  to a Gaussian in the latent space as follows:

$$\boldsymbol{\mu}_{\text{latent}} = \text{FFN}_{\boldsymbol{\mu}}^{\text{down}}(\mathbf{F}_{\text{end}}), \quad \boldsymbol{\sigma}_{\text{latent}} = \text{Softplus}(\text{FFN}_{\boldsymbol{\sigma}}^{\text{down}}(\mathbf{F}_{\text{end}})), \quad (3)$$

where the Softplus ensures  $\boldsymbol{\sigma}_{\text{latent}} > 0$ . We draw  $N_{\text{rep}}$  latent codes  $\mathbf{z}_i \sim \mathcal{N}(\boldsymbol{\mu}_{\text{latent}}, \boldsymbol{\sigma}_{\text{latent}}^2)$  and decode them with an up-projection FFN, obtaining the predictive parameters  $(\boldsymbol{\mu}_{\text{rec},i}, \boldsymbol{\sigma}_{\text{rec},i})$  analogous to Eq. (3). The conditional likelihood of the feature can be therefore formulated as:

$$p(\mathbf{F}_{\text{end}} | \mathbf{z}_i) = \mathcal{N}(\mathbf{F}_{\text{end}}; \boldsymbol{\mu}_{\text{rec},i}, \boldsymbol{\sigma}_{\text{rec},i}^2) = \frac{1}{\boldsymbol{\sigma}_{\text{rec},i} \sqrt{2\pi}} \exp\left[-\frac{\|\mathbf{F}_{\text{end}} - \boldsymbol{\mu}_{\text{rec},i}\|^2}{2\boldsymbol{\sigma}_{\text{rec},i}^2}\right]. \quad (4)$$

Averaging Eq. (4) over  $N_{\text{rep}}$  samples estimates the reconstruction probability  $p_{\text{rec}}(\mathbf{F}_{\text{end}})$  for task  $i$ .

**Primitive bank construction.** After the VAE convergence, we collect the most recent  $T$  training instances of task  $i$ , compute their  $p_{\text{rec}}(\mathbf{F}_{\text{end}})$ , and record the empirical mean and standard deviation, representing the primitive distribution of task  $i$ . Consequently, we construct a key-value bank  $B = \{(\text{primitive}_i, \text{router}_i) \mid i = 1, \dots, N\}$ , where each key stores the probability statistics and each value is the frozen router produced by PGKE.

**Task-agnostic inference.** For an input, we obtain its feature  $\mathbf{F}_{\text{end}}$ , evaluate and z-score normalise its reconstruction probability under every primitive in  $B$ , yielding scores  $\{\hat{p}^{(i)}\}_{i=1}^N$ . The task is inferred as  $i^* = \arg \max_i \hat{p}^{(i)}$ , and the corresponding router  $(i^*)$  is activated for subsequent processing.

### 3.3 Training Objective

For PTL, the training loss consists of two components: the reconstruction loss and the Kullback-Leibler (KL) divergence between the posterior distribution and the prior distribution of the latent space. The reconstruction loss can be measured by the negative reconstruction probability:

$$\mathcal{L}_{\text{rec}} = -p_{\text{rec}}(\mathbf{F}_{\text{end}}). \quad (5)$$

We follow the common setting of VAE that the prior distribution of the latent space is  $\mathcal{N}(\mathbf{0}, \mathbf{1})$ [29]. The posterior distribution of the latent space is  $\mathcal{N}(\boldsymbol{\mu}_{\text{latent}}, \boldsymbol{\sigma}_{\text{latent}}^2)$ . The KL divergence  $\mathcal{L}_{\text{KL}}$  is calculated between the two distributions. For PGKE, similar to most large language models, we employ the next token prediction training schema and utilize a cross-entropy loss  $\mathcal{L}_{\text{CE}}$ . Besides, referring to [18], we also add a weight balance loss  $\mathcal{L}_{\text{aux}}$  for MoE training. Finally, the complete loss is composed of a weighted sum of these components:

$$\mathcal{L}_{\text{total}} = \mathcal{L}_{\text{CE}} + \lambda \mathcal{L}_{\text{KL}} + \eta \mathcal{L}_{\text{rec}} + \kappa \mathcal{L}_{\text{aux}}, \quad (6)$$

where  $\lambda$ ,  $\eta$  and  $\kappa$  are the weighting coefficients for loss balance.

## 4 Experiments and Discussions

### 4.1 Setups and Implementation Details.

**Datasets.** We conducted experiments on the datasets included in the CoIN [7] benchmark, which encompasses a series of eight VQA tasks. These tasks include RefCOCO (Ref) [28], ImageNet [14], TextVQA (TQA) [56], VizWiz [19], SciencQA (SQA) [50], among others. Each task varies in terms of the number of data samples, stylistic features, and domain characteristics. The training set comprises a total of 569k samples, while the testing set contains 261k samples.

**Metrics.** We adopt the metric introduced in CoIN [7], which measures the discrepancy between the model’s output and the ground truth. For assessing the model’s overall forgetting performance

Table 1: A comprehensive comparison with baseline models and other continual learning approaches built upon LLaVA is detailed in the subsequent section. *Immediate* means performance after immediate task training. *Last* means performance after the last task training. *Mean* means the average accuracy on all eight tasks.

Setting	Method	Accuracy on Each Task								Mean $\uparrow$	BWT $\uparrow$
		SQA	TQA	ImageNet	GQA	VizWiz	Ref	VQAv2	OCR-VQA		
Multitask	MoELoRA	75.01	58.90	96.44	58.15	56.73	27.54	64.04	47.81	60.58	–
	LoRA	75.01	58.36	96.08	53.87	56.54	18.32	63.23	53.96	59.42	–
	MoELoRA	78.97	61.01	97.01	56.24	56.30	20.63	66.10	60.57	62.10	–
	EWC [51]	79.23	61.26	96.91	56.43	60.04	19.21	66.00	60.44	62.44	–
	LWF [36]	78.83	61.57	97.07	56.75	53.48	20.57	65.27	61.10	61.83	–
Ours	<b>79.01</b>	<b>59.94</b>	<b>96.85</b>	<b>56.43</b>	<b>57.44</b>	<b>25.63</b>	<b>65.15</b>	<b>62.01</b>	<b>62.81</b>	–	
Last	LoRA	68.50	42.01	34.65	40.39	40.87	3.60	55.29	53.96	42.41	-17.01
	MoELoRA	67.06	48.16	36.22	41.83	41.00	2.62	<b>56.48</b>	60.57	44.24	-17.86
	EWC [51]	60.25	47.92	30.36	41.33	31.12	4.53	56.31	60.44	41.53	-20.90
	LWF [36]	65.15	49.46	32.52	41.05	37.88	4.81	56.20	<b>61.10</b>	43.51	-18.31
	Ours	<b>77.55</b>	<b>58.17</b>	<b>94.50</b>	<b>48.91</b>	<b>55.45</b>	<b>23.40</b>	56.40	59.44	<b>59.23</b>	<b>-3.58</b>

across all tasks, we utilized Backward Transfer (BWT), which evaluates the model’s performance on all previous tasks after it is trained on the last task, specifically quantifies the extent of forgetting, offering insights into the model’s ability to retain knowledge from previous tasks.

**Baseline Models.** Following CoIN [7], we also adopted several other representative methods based on architecture and regularization, including EWC [51], LwF [36], as baselines to compare with our proposed method. To ensure a fair comparison, we align factors that could potentially affect fairness, such as the rank of LoRA and the data used for initializing the model. For more details, refer to CoIN.

**Training Details.** Our network is built upon the pretrained model of LLaVA as our backbone model. It is important to emphasize that throughout all our training processes, only the newly added experts and the corresponding routers are trained, while other existing components remain frozen. New expert weights are copied from the experts selected by Task Probe, and new router weights are initialized by copying old routers and concatenating them with random linear weights. While training Task-Probe, we randomly select 10% data from each train dataset and utilize them to generate probability of each layer to extend. Please refer to the Appendix for details of the network structures, hyperparameters, and any other implementation details.

## 4.2 Quantitative Results on Continual Learning Benchmark

As presented in Table 1, we conducted an evaluation on the CoIN [7] Benchmark. Compared with other methods, our model demonstrates outstanding performance in both immediate and post-last-task training phases, while the average number of trainable parameters in our model is only 43.96M, more details can be found in the appendix. This significantly reduces the training cost. In the setting of *Last*, our method significantly outperforms previous approaches, demonstrating its strong capability in mitigating forgetting, especially on the ImageNet dataset, our method achieves an improvement of nearly 85%. Additionally, it is observed that on the OCR-VQA dataset, all other methods yield consistent results across both settings. However, when a new task is introduced, these methods exhibit substantial forgetting on this dataset, as evidenced by the performance in the first seven tasks. In contrast, our method maintains a stable performance of approximately 59%, showcasing its robustness against forgetting. Besides, as evident from the left of Table 2, employing our proposed method for expert extension and training yields superior results on most tasks compared to the outcomes of training without expanding experts and unfreezing the previously frozen experts.

## 4.3 Ablation Study and Analysis

*Where should the experts be extended?* When expanding experts, a common practice is to add experts to every layer for each task [64]. However, we argue that this approach is inefficient due to significant knowledge overlap between tasks, which leads to parameter redundancy. To validate the

Table 2: **Left:** Comparison of forgetting between the Extend and w/o Extend models. “Extend” freezes original experts and adds new ones using our method, while “w/o Extend” unfreezes all experts and continues training without adding new ones. **Right:** Comparison of expert addition strategies. “Ours” adds experts at selected layers using our method, “Random” adds experts randomly at the same number of layers, and “Every-layer” adds experts to all layers. Param-ratio is the proportion of parameters added by Ours compared to Every-layer.

Dataset	w/o Extend	Extend	Dataset	Random	Every-layer	Ours	Param-ratio
SQA	76.68	<b>77.55</b>	SQA	76.73	<b>80.03</b>	79.01	0.65
TQA	49.42	<b>58.17</b>	TQA	58.87	<b>60.07</b>	59.94	0.812
ImageNet	45.72	<b>94.50</b>	ImageNet	96.75	<b>97.09</b>	96.85	0.75
GQA	44.65	<b>48.91</b>	GQA	<b>57.60</b>	57.28	56.43	0.625
VizWiz	46.79	<b>55.45</b>	VizWiz	54.62	56.52	<b>57.44</b>	0.5
Ref	4.00	<b>23.40</b>	Ref	20.98	<b>31.68</b>	25.63	0.75
VQAv2	<b>58.58</b>	56.40	VQAv2	64.20	64.97	<b>65.15</b>	0.75
OCR-VQA	<b>60.24</b>	59.44	OCR-VQA	56.87	59.78	<b>62.01</b>	0.84
BWT↑	-17.68	<b>-3.58</b>					

Table 3: Comparison of different task orders. “Norm” denotes that we follow CoIN’s training order. “Rev” denotes that we reverse CoIN’s training order. “Rand” denotes that we random shuffle the training order of the CoIN’s datasets.

Setting	Immediate			Last		
	Norm	Rev	Rand	Norm	Rev	Rand
ScienceQA	79.01	<b>79.96</b>	79.63	77.55	78.42	<b>78.48</b>
TextVQA	<b>59.94</b>	58.60	58.51	<b>58.17</b>	56.12	56.01
ImageNet	96.85	<b>96.99</b>	96.89	94.50	<b>94.61</b>	94.55
GQA	56.43	<b>57.88</b>	57.81	48.91	<b>50.32</b>	50.29
VizWiz	57.44	<b>58.76</b>	57.92	55.45	<b>56.77</b>	56.70
Ref	25.63	<b>29.29</b>	29.13	23.40	<b>27.23</b>	27.09
VQAv2	<b>65.15</b>	64.75	64.83	<b>56.40</b>	56.02	56.16
OCR-VQA	<b>62.01</b>	61.27	61.31	<b>59.44</b>	58.72	58.66
Mean ↑	62.81	<b>63.43</b>	63.25	59.23	<b>59.78</b>	59.74
BWT ↑	-	-	-	-3.58	-3.66	<b>-3.51</b>

effectiveness of our PGKE algorithm, as shown in Table 3, we compare several expansion strategies. By comparing the results of Ours and Every-layer, it is evident that our method achieves comparable performance with only 60% of the parameters, even outperforming the every-layer approach on OCR-VQA. Furthermore, the comparison between Random and Ours demonstrates that the positions identified by the task probe are more reasonable, yielding an average performance improvement of 3%-4% under the same training parameter budget, showing the superiority of the PGKE method.

**How does task order influence performance?** We conducted experiments on our method under different training orders across eight datasets of CoIN to verify its robustness to training order. As shown in the table, the forgetting level of our method remains stable across different training orders. This is because the feature extraction and reconstruction of different tasks are independent, same as task routers. Previously trained tasks do not affect the features of subsequent tasks. Additionally, training order has a minimal impact on the method’s immediate performance, though this is not our primary focus. More details will be discussed in the Appendix.

**How many experts should be extended?** Our experiments show that for certain challenging tasks, increasing the number of parameters is crucial, even when added to layers with overlapping knowledge (see the left side of Table 2). To investigate further, we examined how the number of experts per layer affects performance on the Ref and SQA tasks by adding 1, 4, or 8 experts to probe-selected layers (results in Table 4). We found that performance on the more difficult Grounding task improves significantly with more parameters, while the simpler SQA task benefits only marginally. However, due to the distinction between task difficulty and task dissimilarity, we could not develop an end-to-

end method for determining the optimal number of experts based on task difficulty. As a result, we focused on optimizing layer selection and treated the number of experts as a hyperparameter.

**How does the PTL mechanism perform?** To figure out the PTL mechanism, we conducted the following two ablation experiments: 1) **Last** task evaluation: We utilized the router and the corresponding set of experts learned from the last task to evaluate all previous tasks. 2) **Random** task evaluation: We randomly selected a task router and its corresponding set of experts to evaluate all tasks. Results are presented in the left part of Table 5. The last task is excluded from analysis since it is not affected by forgetting. Under these conditions, our PTL method significantly outperforms the other approaches, indicating that our task reconstruction strategy enables PTL to better retain knowledge of past tasks. Additional experiments on feature extraction methods are detailed in the Appendix.

**Can knowledge from previous tasks facilitate new task learning?** In continual learning, beyond mitigating forgetting, it is also important to assess whether prior knowledge facilitates learning new tasks. To this end, we evaluated the model’s forward transfer by comparing it to models trained from scratch on each of the eight tasks, with an equal number of trainable parameters, as shown in the right side of Table 5. Results show that while prior knowledge offers limited benefits for simpler tasks, it significantly accelerates learning on more challenging tasks like Ref and OCRVQA.

Figure 4: Qualitative Results of LLaVA-CMoE.



Table 5: Left: Comparison of different task classification strategies. Right: Knowledge forward transfer ability comparison.

Dataset	Last	Random	Ours	Dataset	Separate	Ours
SQA	73.03	61.92	<b>77.55</b>	SQA	78.97	<b>79.01</b>
TQA	46.82	50.62	<b>58.17</b>	TQA	<b>60.56</b>	59.94
ImageNet	29.68	36.59	<b>94.50</b>	ImageNet	<b>97.05</b>	96.85
GQA	41.81	43.12	<b>48.91</b>	GQA	56.31	<b>56.43</b>
VizWiz	44.32	37.86	<b>55.45</b>	VizWiz	56.20	<b>57.44</b>
Ref	9.92	4.83	<b>23.40</b>	Ref	21.3	<b>25.63</b>
VQAv2	55.13	45.90	<b>56.40</b>	VQAv2	65.01	<b>65.15</b>
OCR	62.01	25.62	<b>59.44</b>	OCR	60.79	<b>62.01</b>

**Qualitative Results.** We qualitatively analyze the model’s outputs. As illustrated in Figure 7, after training on the final task, we randomly sample data from previous tasks and compare results across methods. On ImageNet, our model retains domain-specific knowledge with minimal forgetting, while LLaVA-w/o-MoE relies on pretrained knowledge and produces generic responses. For the Grounding task, our model better preserves knowledge required for non-linguistic generation.

## 5 Conclusion and Discussion

In this paper, we propose LLaVA-CMoE, a continual learning framework comprising two key modules: Probe-Guided Knowledge Extension (PGKE) and Probabilistic Task Locator (PTL). PGKE addresses the inefficiency of continuous parameter expansion by adaptively increasing parameters through probe-guided expert addition. Meanwhile, PTL mitigates catastrophic forgetting in continual learning by modeling task distributions and memorizing the mapping between task distributions and router networks. Qualitative and quantitative results demonstrate that our method remarkably outperforms the existing methods.

**Limitation.** Expert addition is currently limited, as adding experts only to the language model may not fully benefit tasks requiring detailed visual understanding. Additionally, increasing tasks raises storage demands, and existing distillation or merging methods can cause router-related forgetting. We will address these issues in future work.

**Societal impact.** Our method improves continual learning in multimodal models, benefiting applications like education and accessibility. However, increased adaptability may also heighten risks of misuse, underscoring the need for responsible deployment and oversight.

## References

- [1] Nermeen Abou Baker, David Rohrschneider, and Uwe Handmann. Parameter-efficient fine-tuning of large pretrained models for instance segmentation tasks. *Machine Learning and Knowledge Extraction*, 6(4):2783–2807, 2024.
- [2] Jinwon An and Sungzoon Cho. Variational autoencoder based anomaly detection using reconstruction probability, 2015.
- [3] Tom Brown, Benjamin Mann, Nick Ryder, Melanie Subbiah, Jared D Kaplan, Prafulla Dhariwal, Arvind Neelakantan, Pranav Shyam, Girish Sastry, Amanda Askell, et al. Language models are few-shot learners. *Advances in neural information processing systems*, 33:1877–1901, 2020.
- [4] Davide Caffagni, Federico Cocchi, Luca Barsellotti, Nicholas Moratelli, Sara Sarto, Lorenzo Baraldi, Lorenzo Baraldi, Marcella Cornia, and Rita Cucchiara. The revolution of multimodal large language models: A survey. In Lun-Wei Ku, Andre Martins, and Vivek Srikumar, editors, *Findings of the Association for Computational Linguistics: ACL 2024*, pages 13590–13618, Bangkok, Thailand, August 2024. Association for Computational Linguistics.
- [5] Jie Cai, Xin Wang, Chaoyu Guan, Yateng Tang, Jin Xu, Bin Zhong, and Wenwu Zhu. Multi-modal continual graph learning with neural architecture search. In *Proceedings of the ACM Web Conference 2022*, pages 1292–1300, 2022.
- [6] Yuliang Cai, Jesse Thomason, and Mohammad Rostami. Task-attentive transformer architecture for continual learning of vision-and-language tasks using knowledge distillation. *arXiv preprint arXiv:2303.14423*, 2023.
- [7] Cheng Chen, Junchen Zhu, Xu Luo, Hengtao Shen, Jingkuan Song, and Lianli Gao. Coin: A benchmark of continual instruction tuning for multimodal large language models. *Advances in Neural Information Processing Systems*, 37:57817–57840, 2024.
- [8] Wuyang Chen, Yanqi Zhou, Nan Du, Yanping Huang, James Laudon, Zhifeng Chen, and Claire Cui. Lifelong language pretraining with distribution-specialized experts. In *International Conference on Machine Learning*, pages 5383–5395. PMLR, 2023.
- [9] Yifan Chen, Devamanyu Hazarika, Mahdi Namazifar, Yang Liu, Di Jin, and Dilek Hakkani-Tur. Empowering parameter-efficient transfer learning by recognizing the kernel structure in self-attention. In *Findings of the Association for Computational Linguistics: NAACL 2022*, pages 1375–1388, 2022.
- [10] Zeren Chen, Ziqin Wang, Zhen Wang, Huayang Liu, Zhenfei Yin, Si Liu, Lu Sheng, Wanli Ouyang, Yu Qiao, and Jing Shao. Octavius: Mitigating task interference in mllms via lora-moe. *arXiv preprint arXiv:2311.02684*, 2023.
- [11] Zhiyuan Chen and Bing Liu. Continual learning and catastrophic forgetting. In *Lifelong Machine Learning*, pages 55–75. Springer, 2018.
- [12] Riccardo Del Chiaro, Bartłomiej Twardowski, Andrew D. Bagdanov, and Joost van de Weijer. Ratt: Recurrent attention to transient tasks for continual image captioning, 2020.
- [13] Aakanksha Chowdhery, Sharan Narang, Jacob Devlin, Maarten Bosma, Gaurav Mishra, Adam Roberts, Paul Barham, Hyung Won Chung, Charles Sutton, Sebastian Gehrmann, et al. Palm: Scaling language modeling with pathways. *Journal of Machine Learning Research*, 24(240):1–113, 2023.
- [14] Jia Deng, Wei Dong, Richard Socher, Li-Jia Li, Kai Li, and Li Fei-Fei. Imagenet: A large-scale hierarchical image database. In *2009 IEEE Conference on Computer Vision and Pattern Recognition*, pages 248–255, 2009.
- [15] Marco D’Alessandro, Alberto Alonso, Enrique Calabrés, and Mikel Galar. Multimodal parameter-efficient few-shot class incremental learning. In *2023 IEEE/CVF International Conference on Computer Vision Workshops (ICCVW)*, page 3385–3395. IEEE, October 2023.

- [16] Ali Edalati, Marzieh Tahaei, Ivan Kobyzev, Vahid Partovi Nia, James J Clark, and Mehdi Rezagholizadeh. Krona: Parameter efficient tuning with kronecker adapter. *arXiv preprint arXiv:2212.10650*, 2022.
- [17] Mehrdad Farajtabar, Navid Azizan, Alex Mott, and Ang Li. Orthogonal gradient descent for continual learning. In *International conference on artificial intelligence and statistics*, pages 3762–3773. PMLR, 2020.
- [18] William Fedus, Barret Zoph, and Noam Shazeer. Switch transformers: Scaling to trillion parameter models with simple and efficient sparsity, 2022.
- [19] Danna Gurari, Qing Li, Abigale J. Stangl, Anhong Guo, Chi Lin, Kristen Grauman, Jiebo Luo, and Jeffrey P. Bigham. VizWiz Grand Challenge: Answering Visual Questions from Blind People . In *2018 IEEE/CVF Conference on Computer Vision and Pattern Recognition (CVPR)*, pages 3608–3617, Los Alamitos, CA, USA, June 2018. IEEE Computer Society.
- [20] Zeyu Han, Chao Gao, Jinyang Liu, Jeff Zhang, and Sai Qian Zhang. Parameter-efficient fine-tuning for large models: A comprehensive survey, 2024.
- [21] Demis Hassabis, Dharshan Kumaran, Christopher Summerfield, and Matthew Botvinick. Neuroscience-inspired artificial intelligence. *Neuron*, 95(2):245–258, 2017.
- [22] Jinghan He, Haiyun Guo, Ming Tang, and Jinqiao Wang. Continual instruction tuning for large multimodal models, 2023.
- [23] Neil Houlsby, Andrei Giurgiu, Stanislaw Jastrzebski, Bruna Morrone, Quentin De Laroussilhe, Andrea Gesmundo, Mona Attariyan, and Sylvain Gelly. Parameter-efficient transfer learning for nlp. In *International Conference on Machine Learning*, pages 2790–2799. PMLR, 2019.
- [24] Edward J Hu, Yelong Shen, Phillip Wallis, Zeyuan Allen-Zhu, Yuanzhi Li, Shean Wang, Lu Wang, and Weizhu Chen. LoRA: Low-rank adaptation of large language models. In *International Conference on Learning Representations*, 2022.
- [25] Saurav Jha, Dong Gong, and Lina Yao. Clap4clip: Continual learning with probabilistic finetuning for vision-language models, 2024.
- [26] Albert Q. Jiang, Alexandre Sablayrolles, Antoine Roux, Arthur Mensch, Blanche Savary, Chris Bamford, Devendra Singh Chaplot, Diego de las Casas, Emma Bou Hanna, Florian Bressand, Gianna Lengyel, Guillaume Bour, Guillaume Lample, L lio Renard Lavaud, Lucile Saulnier, Marie-Anne Lachaux, Pierre Stock, Sandeep Subramanian, Sophia Yang, Szymon Antoniak, Teven Le Scao, Th ophile Gervet, Thibaut Lavril, Thomas Wang, Timoth e Lacroix, and William El Sayed. Mixtral of experts, 2024.
- [27] Rabeeh Karimi Mahabadi, James Henderson, and Sebastian Ruder. Compacter: Efficient low-rank hypercomplex adapter layers. *Advances in Neural Information Processing Systems*, 34:1022–1035, 2021.
- [28] Sahar Kazemzadeh, Vicente Ordonez, Mark Matten, and Tamara Berg. ReferItGame: Referring to objects in photographs of natural scenes. In Alessandro Moschitti, Bo Pang, and Walter Daelemans, editors, *Proceedings of the 2014 Conference on Empirical Methods in Natural Language Processing (EMNLP)*, pages 787–798, Doha, Qatar, October 2014. Association for Computational Linguistics.
- [29] Diederik P. Kingma and Max Welling. Auto-encoding variational bayes. *CoRR*, abs/1312.6114, 2013.
- [30] James Kirkpatrick, Razvan Pascanu, Neil Rabinowitz, Joel Veness, Guillaume Desjardins, Andrei A. Rusu, Kieran Milan, John Quan, Tiago Ramalho, Agnieszka Grabska-Barwinska, Demis Hassabis, Claudia Clopath, Dharshan Kumaran, and Raia Hadsell. Overcoming catastrophic forgetting in neural networks. *Proceedings of the National Academy of Sciences*, 114(13):3521–3526, March 2017.

- [31] Mingrui Lao, Nan Pu, Yu Liu, Zhun Zhong, Erwin M. Bakker, Nicu Sebe, and Michael S. Lew. Multi-domain lifelong visual question answering via self-critical distillation. In *Proceedings of the 31st ACM International Conference on Multimedia*, MM '23, page 4747–4758, New York, NY, USA, 2023. Association for Computing Machinery.
- [32] Stan Weixian Lei, Difei Gao, Jay Zhangjie Wu, Yuxuan Wang, Wei Liu, Mengmi Zhang, and Mike Zheng Shou. Symbolic replay: Scene graph as prompt for continual learning on vqa task. In *Proceedings of the AAAI Conference on Artificial Intelligence*, volume 37, pages 1250–1259, 2023.
- [33] Dmitry Lepikhin, HyounJoong Lee, Yuanzhong Xu, Dehao Chen, Orhan Firat, Yanping Huang, Maxim Krikun, Noam Shazeer, and Zhifeng Chen. Gshard: Scaling giant models with conditional computation and automatic sharding, 2020.
- [34] Junnan Li, Dongxu Li, Silvio Savarese, and Steven C. H. Hoi. Blip-2: Bootstrapping language-image pre-training with frozen image encoders and large language models. In *International Conference on Machine Learning*, 2023.
- [35] Xiang Lisa Li and Percy Liang. Prefix-tuning: Optimizing continuous prompts for generation. *arXiv preprint arXiv:2101.00190*, 2021.
- [36] Zhizhong Li and Derek Hoiem. Learning without forgetting. *IEEE transactions on pattern analysis and machine intelligence*, 40(12):2935–2947, 2017.
- [37] Haotian Liu, Chunyuan Li, Qingyang Wu, and Yong Jae Lee. Visual instruction tuning. *Advances in neural information processing systems*, 36:34892–34916, 2023.
- [38] Qidong Liu, Xian Wu, Xiangyu Zhao, Yuanshao Zhu, Derong Xu, Feng Tian, and Yefeng Zheng. When moe meets llms: Parameter efficient fine-tuning for multi-task medical applications. In *Proceedings of the 47th International ACM SIGIR Conference on Research and Development in Information Retrieval*, pages 1104–1114, 2024.
- [39] Xiao Liu, Kaixuan Ji, Yicheng Fu, Weng Tam, Zhengxiao Du, Zhilin Yang, and Jie Tang. P-tuning: Prompt tuning can be comparable to fine-tuning across scales and tasks. In Smaranda Muresan, Preslav Nakov, and Aline Villavicencio, editors, *Proceedings of the 60th Annual Meeting of the Association for Computational Linguistics (Volume 2: Short Papers)*, pages 61–68, Dublin, Ireland, May 2022. Association for Computational Linguistics.
- [40] Xiao Liu, Kaixuan Ji, Yicheng Fu, Weng Lam Tam, Zhengxiao Du, Zhilin Yang, and Jie Tang. P-tuning v2: Prompt tuning can be comparable to fine-tuning universally across scales and tasks. *arXiv preprint arXiv:2110.07602*, 2021.
- [41] David Lopez-Paz and Marc’ Aurelio Ranzato. Gradient episodic memory for continual learning. *Advances in neural information processing systems*, 30, 2017.
- [42] Tongxu Luo, Jiahe Lei, Fangyu Lei, Weihao Liu, Shizhu He, Jun Zhao, and Kang Liu. Moelora: Contrastive learning guided mixture of experts on parameter-efficient fine-tuning for large language models. *ArXiv*, abs/2402.12851, 2024.
- [43] Basil Mustafa, Carlos Riquelme, Joan Puigcerver, Rodolphe Jenatton, and Neil Houlsby. Multi-modal contrastive learning with limoe: the language-image mixture of experts. *Advances in Neural Information Processing Systems*, 35:9564–9576, 2022.
- [44] Yuxin Peng, Jinwei Qi, Zhaoda Ye, and Yunkan Zhuo. Hierarchical visual-textual knowledge distillation for life-long correlation learning. *Int. J. Comput. Vision*, 129(4):921–941, April 2021.
- [45] Lucas Pinheiro Cinelli, Matheus Araújo Marins, Eduardo Ant3nio Barros da Silva, and S3rgio Lima Netto. Variational autoencoder. In *Variational methods for machine learning with applications to deep networks*, pages 111–149. Springer, 2021.
- [46] Yunchen Pu, Zhe Gan, Ricardo Henao, Xin Yuan, Chunyuan Li, Andrew Stevens, and Lawrence Carin. Variational autoencoder for deep learning of images, labels and captions. *Advances in neural information processing systems*, 29, 2016.

- [47] Zi Qian, Xin Wang, Xuguang Duan, Pengda Qin, Yuhong Li, and Wenwu Zhu. Decouple before interact: Multi-modal prompt learning for continual visual question answering. In *Proceedings of the IEEE/CVF International Conference on Computer Vision (ICCV)*, pages 2953–2962, October 2023.
- [48] Alec Radford, Jong Wook Kim, Chris Hallacy, Aditya Ramesh, Gabriel Goh, Sandhini Agarwal, Girish Sastry, Amanda Askell, Pamela Mishkin, Jack Clark, Gretchen Krueger, and Ilya Sutskever. Learning transferable visual models from natural language supervision. In *International Conference on Machine Learning*, 2021.
- [49] Carlos Riquelme, Joan Puigcerver, Basil Mustafa, Maxim Neumann, Rodolphe Jenatton, André Susano Pinto, Daniel Keysers, and Neil Houlsby. Scaling vision with sparse mixture of experts. *Advances in Neural Information Processing Systems*, 34:8583–8595, 2021.
- [50] Tanik Saikh, Tirthankar Ghosal, Amish Mittal, Asif Ekbal, and Pushpak Bhattacharyya. Scienceqa: A novel resource for question answering on scholarly articles. *International Journal on Digital Libraries*, 23(3):289–301, 2022.
- [51] Jonathan Schwarz, Wojciech Czarnecki, Jelena Luketina, Agnieszka Grabska-Barwinska, Yee Whye Teh, Razvan Pascanu, and Raia Hadsell. Progress & compress: A scalable framework for continual learning. In *International conference on machine learning*, pages 4528–4537. PMLR, 2018.
- [52] Joan Serra, Dídac Surís, Marius Miron, and Alexandros Karatzoglou. Overcoming catastrophic forgetting with hard attention to the task, 2018.
- [53] Noam Shazeer, Azalia Mirhoseini, Krzysztof Maziarz, Andy Davis, Quoc V. Le, Geoffrey E. Hinton, and Jeff Dean. Outrageously large neural networks: The sparsely-gated mixture-of-experts layer. *arXiv: Learning*, Jan 2017.
- [54] Sheng Shen, Zhewei Yao, Chunyuan Li, Trevor Darrell, Kurt Keutzer, and Yuxiong He. Scaling vision-language models with sparse mixture of experts. *arXiv preprint arXiv:2303.07226*, 2023.
- [55] Haizhou Shi, Zihao Xu, Hengyi Wang, Weiyi Qin, Wenyuan Wang, Yibin Wang, Zifeng Wang, Sayna Ebrahimi, and Hao Wang. Continual learning of large language models: A comprehensive survey. *arXiv preprint arXiv:2404.16789*, 2024.
- [56] Amanpreet Singh, Vivek Natarajan, Meet Shah, Yu Jiang, Xinlei Chen, Dhruv Batra, Devi Parikh, and Marcus Rohrbach. Towards VQA models that can read. In *IEEE Conference on Computer Vision and Pattern Recognition, CVPR 2019, Long Beach, CA, USA, June 16-20, 2019*, pages 8317–8326. Computer Vision Foundation / IEEE, 2019.
- [57] Fuchun Sun, Huaping Liu, Chao Yang, and Bin Fang. Multimodal continual learning using online dictionary updating. *IEEE Transactions on Cognitive and Developmental Systems*, 13(1):171–178, 2021.
- [58] Hugo Touvron, Louis Martin, Kevin Stone, Peter Albert, Amjad Almahairi, Yasmine Babaei, Nikolay Bashlykov, Soumya Batra, Prajjwal Bhargava, Shruti Bhosale, et al. Llama 2: Open foundation and fine-tuned chat models. *arXiv preprint arXiv:2307.09288*, 2023.
- [59] Renzhi Wang and Piji Li. Lemoe: Advanced mixture of experts adaptor for lifelong model editing of large language models. *arXiv preprint arXiv:2406.20030*, 2024.
- [60] Yabin Wang, Zhiwu Huang, and Xiaopeng Hong. S-prompts learning with pre-trained transformers: An occam’s razor for domain incremental learning, 2023.
- [61] Jiayang Wu, Wensheng Gan, Zefeng Chen, Shicheng Wan, and Philip S. Yu. Multimodal Large Language Models: A Survey. In *2023 IEEE International Conference on Big Data (BigData)*, pages 2247–2256, Los Alamitos, CA, USA, December 2023. IEEE Computer Society.
- [62] Tongtong Wu, Linhao Luo, Yuan-Fang Li, Shirui Pan, Thuy-Trang Vu, and Gholamreza Haffari. Continual learning for large language models: A survey, 2024.

- [63] Rui Yang, Shuang Wang, Huan Zhang, Siyuan Xu, YanHe Guo, Xiutiao Ye, Biao Hou, and Licheng Jiao. Knowledge decomposition and replay: A novel cross-modal image-text retrieval continual learning method. In *Proceedings of the 31st ACM International Conference on Multimedia*, MM '23, page 6510–6519, New York, NY, USA, 2023. Association for Computing Machinery.
- [64] Shu Yang, Muhammad Asif Ali, Cheng-Long Wang, Lijie Hu, and Di Wang. Moral: Moe augmented lora for llms' lifelong learning, 2024.
- [65] Jiazuo Yu, Yunzhi Zhuge, Lu Zhang, Ping Hu, Dong Wang, Huchuan Lu, and You He. Boosting continual learning of vision-language models via mixture-of-experts adapters. In *Proceedings of the IEEE/CVF Conference on Computer Vision and Pattern Recognition*, pages 23219–23230, 2024.
- [66] Qingru Zhang, Minshuo Chen, Alexander Bukharin, Pengcheng He, Yu Cheng, Weizhu Chen, and Tuo Zhao. Adaptive budget allocation for parameter-efficient fine-tuning. In *The Eleventh International Conference on Learning Representations*, 2022.
- [67] Junhao Zheng, Qianli Ma, Zhen Liu, Binquan Wu, and Huawen Feng. Beyond anti-forgetting: Multimodal continual instruction tuning with positive forward transfer, 2024.
- [68] Zangwei Zheng, Mingyu Ma, Kai Wang, Ziheng Qin, Xiangyu Yue, and Yang You. Preventing zero-shot transfer degradation in continual learning of vision-language models. *2023 IEEE/CVF International Conference on Computer Vision (ICCV)*, pages 19068–19079, 2023.
- [69] Shanshan Zhong, Shanghua Gao, Zhongzhan Huang, Wushao Wen, Marinka Zitnik, and Pan Zhou. Moextend: Tuning new experts for modality and task extension. In *Proceedings of the 62nd Annual Meeting of the Association for Computational Linguistics (Volume 4: Student Research Workshop)*, 2024.
- [70] Yaoming Zhu, Jiangtao Feng, Chengqi Zhao, Mingxuan Wang, and Lei Li. Counter-interference adapter for multilingual machine translation. *arXiv preprint arXiv:2104.08154*, 2021.

# A Technical Appendices and Supplementary Material

## A.1 More Results

**Visualization of PTL mechanism.** We evaluated the PTL mechanism on test data across eight tasks, and the results are shown in Figure 5. As observed from the test results, the PTL mechanism achieves localization accuracies exceeding 80% on five tasks: ScienceQA, ImageNet, VizWiz, Grounding and OCR-VQA. Besides, we can also find that the localization performance on the remaining three tasks, GQA, TextVQA, and VQAv2, is relatively weaker compared to the other five tasks. Through our analysis, this is attributed to the significant overlap in the features of images and questions across these tasks. For instance, GQA and VQAv2 share high similarities in terms of question formats, image content, and styles, which leads to a substantial portion of VQAv2 samples being “mislocalized” to the GQA task.



Figure 5: **Confusion Matrix of PTL.** This figure illustrates the localization performance of the PTL mechanism, where the data in each row and column represent the frequency with which the test data corresponding to the task represented by the column is assigned to the task represented by the row.

**Impact of different selection of PTL feature.** In our main results, we chose the output of the last Decoder layer for classification in the PTL. In Table 6, we also attempted to use the average pooling of outputs from all Decoder layers for classification. Classifying using features from average pooling slightly improved performance on several tasks (SQA, TQA, GQA, VizWiz, Ref), particularly achieving a 7.03% improvement on VQAv2. However, severe performance degradation (~39%) occurred when facing OCR-VQA. We further explored the causes of this decline and found that most samples were classified into the ImageNet task, while a small number of ImageNet samples were classified into OCR-VQA, indicating that average pooling is poor in distinguishing highly similar tasks.

Table 6: Comparison of different feature selection’s influence on model’s performance.

Method	Accuracy on Each Task								Mean↑	BWT↑
	SQA	TQA	ImageNet	GQA	VizWiz	Ref	VQAv2	OCR-VQA		
Last Layer’s feature	77.55	58.17	94.50	48.91	55.45	23.40	56.40	59.44	59.23	-3.58
Pooled feature	77.67	59.19	89.03	51.06	57.03	24.69	63.43	20.68	55.34	-15.31

**Impact of model size.** We conducted experiments on models of varying scales, as delineated in Table 7. Owing to the augmentation in the parameter count of the base model, the performance of the proposed method was further enhanced. Notably, the BWT metric of our approach exhibits a higher value on the 13B model. This phenomenon may be attributed to the fact that the output of the final decoder layer in larger models encompasses more highly abstracted information (hidden-size: 5120 in the 13B model vs. 4096 in the 7B model), which facilitates PTL in achieving superior task classification performance.

Table 7: Comparison of our method on llava-v1.5-7B and llava-v1.5-13B.

Setting	Model Size	Accuracy on Each Task								Mean $\uparrow$	BWT $\uparrow$
		SQA	TQA	ImageNet	GQA	VizWiz	Ref	VQAv2	OCR-VQA		
Immediate	7B	79.01	59.94	96.85	56.43	57.44	25.63	65.15	62.01	62.81	-
	13B	82.32	65.77	98.26	60.41	62.35	30.91	68.75	67.92	67.08	-
Last	7B	77.55	58.17	94.50	48.91	55.45	23.40	56.40	59.44	59.23	-3.58
	13B	80.79	64.82	96.01	52.93	60.86	29.11	62.18	62.27	63.62	-3.46

**Impact of LoRA-rank.** We further investigated the impact of the LoRA rank on our method, as presented in the Table 8. When the LoRA rank was set to 32, there remained a certain margin for performance improvement in the model. However, when the LoRA rank reached 128, the model performance had reached a plateau, with minor performance degradation observed on specific tasks. Therefore, we selected a LoRA rank of 64 as the default setting in our method.

Table 8: Comparison of different lora rank.

Setting	Rank	Accuracy on Each Task								Mean $\uparrow$	BWT $\uparrow$
		SQA	TQA	ImageNet	GQA	VizWiz	Ref	VQAv2	OCR-VQA		
Immediate	32	78.86	59.90	96.32	55.92	57.06	24.17	63.15	60.22	61.95	-
	64	79.01	59.94	96.85	56.43	57.44	25.63	65.15	62.01	62.81	-
	128	79.23	59.54	97.07	57.96	56.03	25.58	65.22	62.33	62.75	-
Last	32	77.32	58.11	94.06	48.44	55.07	22.08	54.02	57.80	58.36	-3.59
	64	77.55	58.17	94.50	48.91	55.45	23.40	56.40	59.44	59.23	-3.58
	128	77.70	57.76	94.59	50.06	54.12	23.11	56.49	59.66	59.19	-3.56

**Parameter comparsion.** We tabulated the number of parameters for different methods, as shown in Table 9. It is worth noting that the LoRA method we compared only adds LoRA matrices to the up-proj layer. Although the LoRA method has the fewest trainable parameters, it exhibits poor anti-forgetting performance. Our method adaptively adds experts based on task differences, significantly enhancing anti-forgetting capabilities while maintaining minimal parameter growth. The changes in trainable parameters across different tasks are illustrated in Figure 6.

**Qualitative Results.** We qualitatively analyze the model’s outputs. As illustrated in Figure 7, after training on the final task, we randomly sample data from previous tasks and compare results across methods. On ImageNet, our model retains domain-specific knowledge with minimal forgetting, while MoELoRA and other methods rely on pretrained knowledge and produces generic responses. For the Ref task, our model better preserves knowledge required for non-linguistic generation.

**Performance over tasks.** We evaluate our methods’ performance during the entire training process. As shown in Table 10, our approach maintains excellent anti-forgetting capability after training on sequential tasks, particularly on the SQA, TQA, ImageNet, VizWiz, and Ref datasets. By comparison, PTL exhibits slightly weaker performance on the VQAv2 and GQA datasets due to a slight classification confusion issue. Nevertheless, its performance remains comparable to or better than existing methods, as demonstrated in our main manuscript.

Table 9: Comparison of the average trainable parameters (M) over eight datasets, and performance between LoRA, MoELoRA, EWC, LWF and Ours.

Metrics	LoRA	MoELoRA	EWC	LWF	Ours
#Trainable Parameters per Task	31M	62M	62M	62M	43.96M
Mean $\uparrow$	42.41	44.24	41.53	43.51	59.23
BWT $\uparrow$	-17.01	-17.86	-20.90	-18.31	-3.58

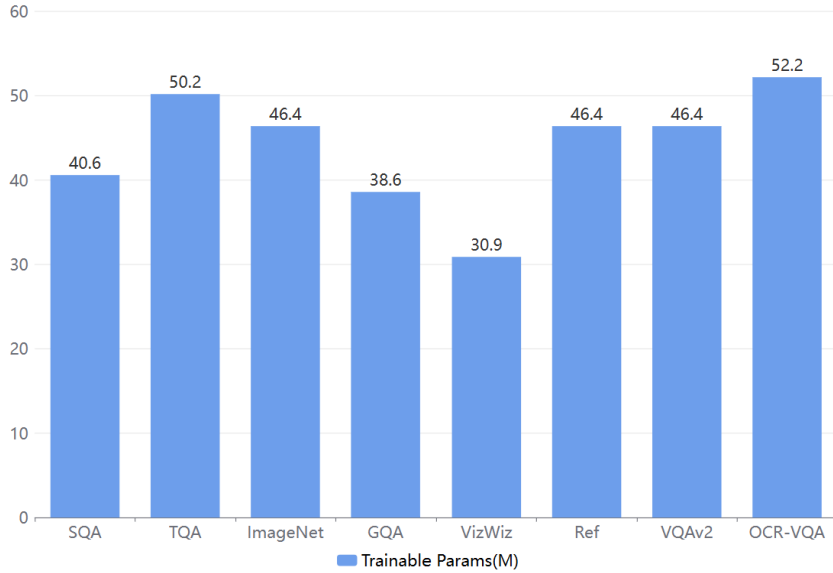


Figure 6: The added trainable parameters on eight tasks.



Figure 7: We randomly select five datasets, which are relatively prone to forgetting, and visualized the results of the two models for comparison.

## A.2 Training Details

We train the model using  $8 \times$  H20 GPUs. It takes 2 hours to train the initial eight experts, followed by 15 hours for the continual learning process. Throughout the training, we set the warmup ratio to

Table 10: The performance on eight datasets during sequential training. Training order: SQA → TQA → ImageNet → GQA → VizWiz → Ref → VQAv2 → OCR-VQA.

Training Dataset	Accuracy on Each Task							
	SQA	TQA	ImageNet	GQA	VizWiz	Ref	VQAv2	OCR-VQA
SQA	79.01	-	-	-	-	-	-	-
TQA	79.01	59.94	-	-	-	-	-	-
ImageNet	79.01	59.71	96.85	-	-	-	-	-
GQA	79.00	59.28	96.31	56.43	-	-	-	-
VizWiz	78.21	58.59	95.13	55.86	57.44	-	-	-
Ref	78.21	58.58	95.12	54.40	57.42	25.63	-	-
VQAv2	77.73	58.31	94.51	49.86	56.31	24.02	65.15	-
OCR-VQA	77.55	58.17	94.50	48.91	55.45	23.40	56.40	62.01

0.03, use the AdamW optimizer, and employ torch BF16 precision with DeepSpeed stage zero2. The rank of LoRA experts is set to 64, the rank alpha to 128, and the global batch size to 128. We assign a weight of  $1e-3$  to the load balancing loss of the router, the KL divergence loss, and the reconstruction loss. For training the normal experts, we use a learning rate of  $2e-4$ , and during the probe experts training, we increase the learning rate to  $3e-4$ .